Journal of Fluorescence
https://doi.org/10.1007/s10895-020-02513-2

ORIGINAL ARTICLE

Design and Synthesis of New Porphyrin Analogues as Potent Photosensitizers for Photodynamic Therapy: Spectroscopic Approach

Prasad G. Mahajan[1] · Nilam C. Dige[2] · Balasaheb D. Vanjare[1] · Chong-Hyeak Kim[3] · Sung-Yum Seo[2] · Ki Hwan Lee[1]

Received: 10 December 2019 / Accepted: 14 February 2020

Abstract

New porphyrin analogues have been designed and synthesized using pyrrole, various aldehydes and propionic acid. The formation of desired compounds was analyzed by utilizing the spectral analysis such as IR, NMR and Mass spectroscopy. The studies on absorption and fluorescence emission of synthesized porphyrins were used to evaluate photophysical characteristics such as molar excitation coefficient and Stokes shift. The estimated values of fluorescence lifetime and fluorescence quantum yield of synthesized porphyrins were found to be variable due to the presence of change in the electron donating and withdrawing characters. The efficiency of generation of singlet oxygen by each synthesized porphyrin as photosensitizer was measured in terms of singlet oxygen quantum yield through photooxidation of 9,10-dimethylantharacene. The obtained singlet oxygen quantum yield values were found to be higher in case of porphyrins those have more electron withdrawing characters rather than donating characters as compared to reference 5,10,15,20-tetraphenylporphyrin (H_2TPP). The singlet oxygen quantum yield values of synthesized porphyrins varied from 0.52 to 0.66. Pleasingly, some of synthesized porphyrins are found to be photostable and competent to discover as PDT agents as compared to reference H_2TPP.

Keywords Porphyrin analogues · Photosensitizers · Photophysical properties · Photodynamic therapy · Singlet oxygen

Introduction

Cancer is one of the leading death cause in the world nowadays. The development of various therapies and discoveries in cancer cell resistance drugs is the research area of interest in current scientific society for the healthy lifestyle [1–3]. Many illnesses are healed by using immunotherapy and photodynamic therapy (PDT). Amongst these two therapies, PDT is widely used because of their acute action and application with minimum side impacts [4–5]. PDT is prime preferred medication when dealing with the therapy used for fatal esophageal tumors, head cancers and lung carcinoma [6]. The basic principle of PDT is the combination of chemical photosensitizer with specific wavelength of light and can be used for the treatment of cancers. The applicability of PDT is advantageous over the traditional cancer remedies such as radiation therapy, chemo-therapy and mainly surgical treatments. The *in situ* damage of networks of cancer tumor is possible only when suitable photosensitizer get excited by light of specific wavelength which capable to produce reactive oxygen species (ROS) [7–8]. The literature review focuses mainly on tetrapyrrole macrocycles cored organic compounds as suitable photosensitizers. Such tetrapyrrole structures mainly contains the synthetic organic compounds such as porphyrins, photofrin, foscan and chlorin [9–10]. The traditional PDT agents could hurdle in the medicinal operation through restriction in selection of tumor site, phototoxicity and inequitable biodistribution [9]. To overcome such disadvantages acquired by traditional agents or therapies, advanced PDT involves the formation of fluorescence signal as well as cytotoxic singlet oxygen when exposed to specific light. Therefore, the design and development of proper PDT agent for the treatment of

Electronic supplementary material The online version of this article (https://doi.org/10.1007/s10895-020-02513-2) contains supplementary material, which is available to authorized users.

✉ Ki Hwan Lee
khlee@kongju.ac.kr

[1] Department of Chemistry, Kongju National University, Gongju, Chungnam 32588, Republic of Korea

[2] Department of Biological Sciences, Kongju National University, Gongju, Chungnam 32588, Republic of Korea

[3] Center for Chemical Analysis, Korea Research Institute of Chemical Technology, Yuseong Daejeon 34114, Republic of Korea

Published online: 22 February 2020

cancer tumors are demanding and challenging subject for the researchers working in the field of chemistry, biology and pharmacy.

Porphyrin plays pivotal role in various fields such as catalysis, sensors, metabolism, electron transfer and photosynthesis [11–13]. The modification in the structure of porphyrin led to change in their properties as far as biomedical point of view concern. It is well known that *meso*-substituted porphyrins of the tetrakis(hydroxyphenyl)porphyrin (THPP) compound retains superior strength and biocompatibility as PDT agents. The existence of various substituents on THPP moiety at *ortho, meta* or *para* position can change their photophysical properties and potency for successful PDT process with efficient generation of singlet oxygen [14]. The superior photophysical properties, selective localization in tumor tissues and amphiphilicity of THPP bearing a variety of substituents on respective positions are capable to deliver the effective treatment on cancer tumors based on PDT. Therefore, design and synthesis of *meso*-substituted porphyrin (THPP) based new analogues for potent PDT application was the main idea and motivation behind the current research work.

In the present investigation, we have designed and synthesized new porphyrin analogues for their potent applicability as PDT agents. For this purpose, various aldehydes, pyrrole and propionic acid were used as precursors to formulate the target compounds. The prepared porphyrin analogues are highly fluorescent and capable for the generation of singlet oxygen when exposed to specific light through excitation process. The photophysical properties such as absorption, fluorescence emission, fluorescence quantum yield and fluorescence lifetime of all synthesized porphyrin analogues were investigated. The studies on photooxidation of 9,10-dimethyl anthracene (DMA) using synthesized porphyrin analogues gave significant values of singlet oxygen quantum yield. In an overall, it concludes that the synthesized porphyrin analogues in present study can be used as PDT agents which shows excellent photophysical properties along with capacity to generate singlet oxygen.

Experimental

Chemicals

5,10,15,20-tetraphenylporphyrin (H_2TPP), pyrrole, various aldehydes and 9,10-Di-methylanthracene (DMA) were obtained from Sigma Aldrich, Korea. The analytical grade dimethyl formamide (DMF), di-chloromethane, methanol and propionic acid were procured from Samchun Chemicals, Korea. Sodium sulphate (Na_2SO_4) and sodium hydrogen carbonate ($NaHCO_3$) were purchased from Alfa Aesar.

Instrumentation

The principle analytical techniques such as FT-IR, ^{1}H NMR and mass analysis were performed for the confirmation and desired structural elucidation in case of all synthesized porphyrin analogues. FT-IR spectra of respective compounds were scanned on Frontier IR (Perkin Elmer) spectrometer. ^{1}H NMR (400 MHz) spectra were obtained by using Bruker Avance 400 MHz spectrometer and TMS as an internal standard. The spectrometer of 2795/ZQ2000 (Waters) was employed to record and study the mass spectrum of each synthesized porphyrin analogue in the present investigation. The absorption spectra of synthesized porphyrins were obtained by using a Shimadzu Spectrophotometer. The fluorescence emission spectra were obtained and analyzed on FS-2 fluorescence spectrophotometer (Scinco, Korea). The fluorescence lifetime values were obtained on Time Correlated Single Photon Counting (TCSPC) spectrophotometer (HORIBA-iHR320) and analyzed using DAS6 Data station software available with the instrument.

General Procedure for the Synthesis of New Porphyrin Analogues 3a-3i

The synthetic route followed for the porphyrin analogues **3a-3i** is shown in Scheme 1. The known synthetic methodology was opted for the synthesis of desired porphyrin analogues **3a-3i** with some alteration in the process of synthesis [15–16]. The 250 ml round bottom flask was equipped with a mixture of pyrrole (72.5 mmol) and respective aldehydes **2a-2i** (72.5 mmol) in 100 mL propionic acid followed by reflux condition at 120–130 °C till the completion of respective reaction with required time. The change in the reaction mass and reaction movement were monitored on TLC. After the completion of reaction, it was allowed to cool at room temperature. The floppy reaction mass thus obtained was transferred to separating funnel with sufficient volume of ethyl acetate and distilled water. The ethyl acetate layer was separately collected and further treated with saturated solution of $NaHCO_3$ for 4 times (each time 100 mL saturated $NaHCO_3$) to assure the absence of any acid residue. Finally, the ethyl acetate layer was dried up using anhydrous Na_2SO_4. Thus, received ethyl acetate layer was further vacuum pressured on rotary pump gave crude porphyrin **3a-3i**. The crystallized form of each porphyrin analogue was obtained using dichloromethane-methanol (1:1, *v:v*) as mixed solvent system. Table 1 indicate substituents present in respective porphyrin structure, reaction time, obtained product yield and melting point for porphyrin analogues **3a-3i**.

Spectral Data of Synthesized New Porphyrin Analogues 3a-3i

Tetrakis-5,10,15,20-(2-Hydroxy-5-Iodophenyl)Porphyrin (3a) M.P.: 159–162 °C; **Fig. S1:**IR: 3447, 3226, 3022, 2961,

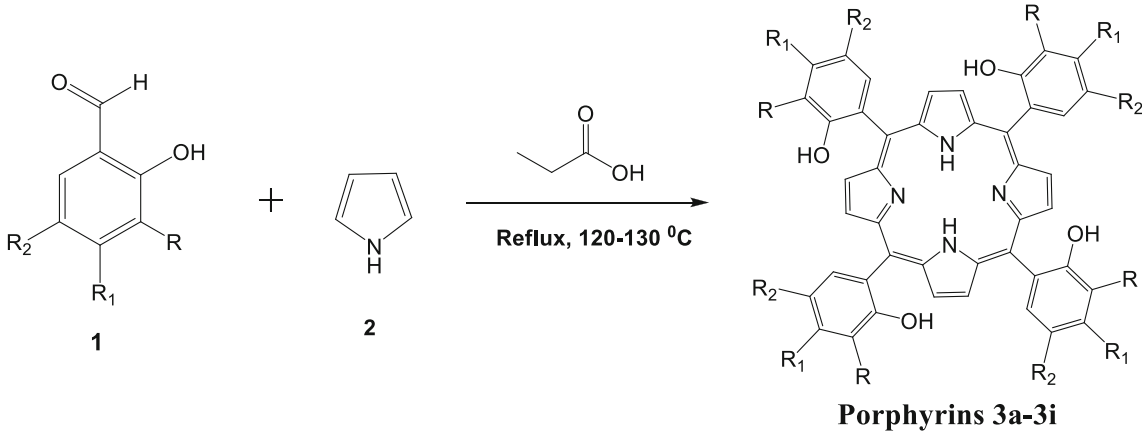

Scheme 1 Synthetic route of new porphyrin analogues **3a-3i**

2299, 1638, 1601, 1580, 1548, 1510, 1486, 1449, 1432, 1395, 1359, 1343, 1282, 1202, 1192, 1142, 1133, 1120,1046, 967, 913, 903, 840, 817, 809, 749, 690, 682 cm^{-1}; **Fig. S2:** ^{1}H-NMR(400 MHz, DMSO-d_6): δ 10.91 (s, 2H, -NH), 10.17 (s, 4H, -OH), 8.80 (s, 1H, -ArH), 8.15–8.24 (q, 2H, -ArH), 7.98 (d, 1H, J = 12 Hz, ArH,), 7.88 (d, 4H, J = 6 Hz, ArH,), 7.78–7.8033 (q, 4H, ArH), 7.18 (t, 2H, J = 6 Hz, ArH,), 6.87 (d, 6H, J = 12 Hz, -ArH,) ppm; **Fig. S3:** LCMS (ESI): 1183.6 (M + 1) *m/z*. Elemental analysis calcd (%) for $C_{44}H_{26}I_4N_4O_4$: C 44.70; H 2.22; I 42.93; N 4.74; O 5.41; found: C 44.69; H 2.21; I 42.92; N 4.76; O 5.42.

Tetrakis-5,10,15,20-(2-Hydroxy-3,5-Dibromophenyl)Porphyrin (3b) M.P.: Above 260 °C; **Fig. S4:**IR: 3448, 3226, 3022, 2297, 1636, 1601, 1581, 1548, 1510, 1487, 1432, 1395, 1360, 1312, 1282, 1202, 1192, 1142, 1133, 1120, 1047, 967, 913, 903, 817, 809, 749, 690, 682 cm^{-1}; **Fig. S5:** ^{1}H-NMR(400 MHz, DMSO-d_6): δ 11.97 (s, 2H, -NH), 9.59–9.73 (m, 4H, -ArH),8.84 (s, 4H, -OH), 8.24 (s, 2H, -ArH), 8.03–8.18 (m, 4H, -ArH), 7.72–7.85 (m, 4H, ArH), 7.55–7.56 (d, 1H, J = 6HZ, -ArH) 7.45 (s, 1H, ArH), 7.28–7.30(d, 1H, J = 12 Hz, -ArH) ppm; **Fig. S6:** LCMS (ESI): 1351.2 (M + 1) *m/z*. Elemental analysis calcd (%) for $C_{44}H_{22}Br_8N_4O_4$: C 40.34; H 1.69; Br 48.80; N 4.28; O 4.89; found: C 40.35; H 1.70; Br 48.79; N 4.26; O 4.90.

Tetrakis-5,10,15,20-(2-Hydroxy-5-Bromophenyl)Porphyrin (3c) M.P.: Above 260 °C; **Fig. S7:**IR: 3446, 3226, 3022, 2299, 1648, 1601, 1581, 1547, 1510, 1486, 1449, 1432, 1395, 1359, 1321, 1282, 1202, 1192, 1142, 1133, 1120, 1046, 967, 913, 903, 817, 809, 749, 690, 682 cm^{-1}; **Fig. S8:** ^{1}H-NMR(400 MHz, DMSO-d_6): δ 11.96 (s, 2H, -NH), 9.96–10.06 (m, 3H, -ArH), 8.85 (s, 4H, -OH), 8.30 (s, 1H, -ArH), 8.03–8.11 (m, 3H, ArH), 7.83–7.85 (m, 4H, -ArH), 7.45–7.52 (t, 2H, J = 18 Hz, -ArH), 7.28–7.31 (m, 5H, -ArH), 7.20–7.25 (m, 2H, ArH) ppm; **Fig. S9:** LCMS (ESI): 995.3 (M + 4) *m/z*. Elemental analysis calcd (%) for $C_{44}H_{26}Br_4N_4O_4$: C 53.15; H 2.64; Br 32.14; N 5.63; O 6.44; found: C 53.14; H 2.63; Br 32.15; N 5.64; O 6.44.

Tetrakis-5,10,15,20-(2-Hydroxy-3,5-Diiodophenyl)Porphyrin (3d) M.P.: 162–166 °C; **Fig. S10:**IR: 3447, 3227, 3022, 2298, 1650, 1600, 1581, 1547, 1395, 1281, 1202, 1192, 1142, 1133, 1120, 967, 913,903, 817, 809, 749, 682 cm^{-1}; **Fig. S11:** ^{1}H-NMR(400 MHz, DMSO-d_6): δ 11.97 (s, 2H, -NH), 9.90 (s, 4H, -OH), 8.79 (s, 4H, -ArH), 8.47 (s, 2H, -ArH), 8.28 (s, 4H,

Table 1 Substituents present in respective porphyrin structure, reaction time, obtained product yield and melting point of porphyrin analogues **3a-3i**

Entry	R	R_1	R_2	Reaction time in min	Product yield (%)	Melting point (^{0} C)
3a	-H	-H	-I	55	41	159–162
3b	-Br	-H	-Br	45	35	Above 260
3c	-H	-H	-Br	55	48	Above 260
3d	-I	-H	-I	35	46	162–166
3e	-H	$-N(C_2H_5)_2$	-H	90	42	115–120
3f	-H	-H	$-CH_3$	70	34	Above 260
3g	$-NO_2$	-H	$-NO_2$	35	39	Above 260
3h	-H	-H	-Cl	55	43	Above 260
3i	$-NO_2$	-H	-H	60	44	221–224

ArH), 8.07–8.11 (m, 2H, ArH), 8.04 (s, 4H, ArH) ppm; **Fig. S12:** LCMS (ESI): 1690.2 (M + 5) *m/z*. Elemental analysis calcd (%) for $C_{44}H_{22}I_8N_4O_4$: C 31.35; H 1.32; I 60.21; N 3.32; O 3.80; found: C 31.36; H 1.33; I 60.20; N 3.33; O 3.78.

Tetrakis-5,10,15,20-(2-Hydroxy-4-N,N′-Diethylphenyl)Porphyrin (3e) M.P.: 115–120 °C; **Fig. S13:**IR: 3447, 3227, 3022, 2298, 1601, 1581, 1554, 1511, 1487, 1448, 1433, 1395, 1282, 1202, 1192,1143, 1133, 1120, 1046, 967, 903, 817, 749, 691, 682 cm^{-1}; **Fig. S14:**^{1}H-NMR(400 MHz, DMSO-d_6): δ 11.26 (s, 2H, -NH), 9.62 (s, 4H, -OH), 7.44(s, 2H, -ArH), 7.42 (s, 2H, -ArH), 6.35–6.36 (m, 6H, -ArH), 6.05(d, 6H, -ArH), 3.39–3.43 (q, 20H, $-NCH_2$), 1.12 (t, 24H, CH_3), ppm; **Fig. S15:** LCMS (ESI): 968.9 (M + 1) *m/z*. Elemental analysis calcd (%) for $C_{60}H_{66}N_8O_4$: C 74.82; H 6.91; N 11.63; O 6.64; found: C 74.84; H 6.90; N 11.64; O 6.62.

Tetrakis-5,10,15,20-(2-Hydroxy-5-Methyphenyl)Porphyrin (3f) M.P.: Above 260 °C; **Fig. S16:**IR: 3453, 3226, 3022, 2309, 1601, 1581, 1553, 1486, 1448, 1395, 1282, 1202, 1192, 1143, 1133, 1120, 1045, 967, 913, 903, 841, 817, 808, 749, 690, 682 cm^{-1}; **Fig. S17:**^{1}H-NMR(400 MHz, DMSO-d_6): δ 10.22 (s, 2H, -NH), 9.28–9.38 (m, 2H, -ArH), 8.77 (s, 4H, -OH), 7.44–7.46 (m, 4H, -ArH), 7.34–7.35 (m, 4H, ArH), 7.21–7.22 (m, 2H, -ArH), 7.20–7.21 (m, 2H, -ArH), 6.90–6.91 (d, 4H, ArH), 1.00 (t, 12H, CH_3) ppm; **Fig. S18:** LCMS (ESI): 735.7 (M + 1) *m/z*. Elemental analysis calcd (%) for $C_{48}H_{38}N_4O_4$: C 78.45; H 5.21; N 7.62; O 8.72; found: C 78.44; H 5.20; N 7.64; O 8.72.

Tetrakis-5,10,15,20-(2-Hydroxy-3,5-Dinitrophenol)Porphyrin (3g) M.P.: Above 260 °C; **Fig. S19:**IR: 3446, 3226, 3022, 2298, 1601, 1581, 1395, 1282, 1202, 1192, 1143, 1133, 1120, 1047, 697, 913, 903, 841, 817, 808, 749, 691, 682 cm^{-1}; **Fig. S20:**^{1}H-NMR(400 MHz, DMSO-d_6): δ 10.47 (s, 2H, -NH), 10.22 (s, 4H, -OH), 9.09 (m, 3H, -ArH), 8.94 (s, 2H, -ArH), 8.76 (s, 2H, ArH), 7.43–7.46 (m, 3H, -ArH), 7.20–7.22 (m, 2H, ArH), 6.90–6.93 (m, 2H, -ArH), 6.52(s, 2H, -ArH) ppm; **Fig. S21:** LCMS (ESI): 1039.8 (M + 1) *m/z*. Elemental analysis calcd (%) for $C_{44}H_{22}N_{12}O_{20}$: C 50.88; H 2.13; N 16.18; O 30.81; found: C 50.90; H 2.14; N 16.16; O 30.80.

Tetrakis-5,10,15,20-(2-Hydroxy-5-Chlorophenyl)Porphyrin (3h) M.P.: Above 260 °C; **Fig. S22:**IR: 3447, 3227, 3022, 2971, 2299, 1599, 1581, 1554, 1486, 1448, 1395, 1282, 1202, 1192, 1143, 1133, 1120, 1046, 967, 913, 903, 842, 816, 808, 749, 690, 682 cm^{-1}; **Fig. S23:**^{1}H-NMR(400 MHz, DMSO-d_6): δ 11.98 (s, 2H, -NH), 9.99 (s, 4H, -OH), 8.82 (s, 2H, -ArH), 8.61 (s, 1H, -ArH), 8.30 (s, 1H, -ArH), 8.24(s, 1H, -ArH), 7.96–7.99 (m, 3H, -ArH), 7.92–7.93 (d, 3H, J = 6 Hz, -ArH,), 7.71–7.73 (m, 2H, ArH), 7.33–7.35 (m, 5H, -ArH), 7.04 (s, 1H, ArH), 6.80 (s, 1H, -ArH) ppm; **Fig. S24:** LCMS (ESI): 817.5 (M + 1) *m/z*. Elemental analysis calcd (%) for $C_{44}H_{26}Cl_4N_4O_4$: C 64.72; H 3.21; Cl 17.37; N 6.86; O 7.84; found: C 64.73; H 3.22; Cl 17.36; N 6.85; O 7.84.

Tetrakis-5,10,15,20-(2-Hydroxy-3-Nitrophenyl)Porphyrin (3i) M.P.: 221–224 °C; **Fig. S25:**IR: 3445, 3213, 3022, 2961, 2298, 1599, 1524, 1486, 1446, 1395, 1282, 1202, 1192, 1143, 1133, 1120, 1046, 967, 913, 903, 808, 745, 691, 682 cm^{-1}; **Fig. S26:**^{1}H-NMR(400 MHz, DMSO-d_6): δ 10.98 (s, 2H, -NH), 10.67 (s, 4H, -OH), 8.88 (s, 2H, -ArH), 8.52–8.53 (d, 2H, -ArH), 8.37–8.39 (m, 3H, ArH), 8.11–8.17 (m, 2H, ArH), 7.86–7.91 (m, 3H, ArH), 7.50–7.53 (t, 3H, J = 6 Hz, -ArH), 7.29–7.30 (d, 1H, J = 6 Hz, -ArH), 7.12–7.15(m, 2H, -ArH), 6.73(s, 1H, -ArH), 6.27 (s, 1H, -ArH) ppm; **Fig. S27:** LCMS (ESI): 859.6 (M + 1) *m/z*. Elemental analysis calcd (%) for $C_{44}H_{26}N_8O_{12}$: C 61.54; H 3.05; N 13.05; O 22.36; found: C 61.53; H3.07; N 13.06; O 22.34.

General Procedure for Absorption, Fluorescence Emission and Fluorescence Lifetime Measurement

The absorption, fluorescence emission and fluorescence lifetime of synthesized porphyrin **3a-3i** were examined in DMF solvent at concentration of 10 μM. The standard solution of 1 mM concentration of each porphyrin **3a-3i** was prepared and further used to prepare desired concentration (10 μM) in DMF solvent. The absorption spectra of compounds were scanned within wavelength range of 350–700 nm. While, excitation wavelength of 420 nm was used to obtain fluorescence emission spectra and to trigger the samples for the fluorescence lifetime studies.

General Procedure for Estimation of Fluorescence Quantum Yield

The 10 μM of respective compounds **3a-3i** solutions were prepared in DMF. All prepared solutions were subjected to undergo deaeration through passing of argon gas for the period of 30 min. For this study, 5,10,15,20-tetraphenylporphyrin (H_2TPP) was used as reference having fluorescence quantum yield (Φ_f) of 0.12 in DMF [16,17]. The fluorescence quantum yield for each synthesized porphyrin analogues **3a-3i** was estimated by using **eq. 1** given below [16,18,19],

$$\Phi_f = \Phi_{f(ref)} \frac{I.A_{ref}}{I_{ref}.\ A} \tag{1}$$

where, Φ_f and $\Phi_{f(ref)}$ denotes the fluorescence quantum yield value of sample under studies and reference H_2TPP, respectively. The area under the curve of emission spectrum of respective compound and H_2TPP represents with I and I_{ref}, respectively. While, A and A_{ref} stands for absorbance of individual compound and absorbance of H_2TPP, respectively.

General Procedure for Estimation of Singlet Oxygen Quantum Yield

To explore the potency of synthesized porphyrins **3a-3i** for the generation of singlet oxygen quantum yield (Φ_Δ), steady state photolysis method was employed. The photooxidation of 9,10-di-methylanthracene was studied comprehensively in the vicinity of porphyrins **3a-3i**. The quartz cuvette equipped with mixture of photosensitizer as 1.5 ml of 100 μM respective compound **3a-3i** in DMF and 1.5 ml of 50 μM DMA in DMF. The selective wavelength was permeated by using optical filter. The change in the absorbance value at 401–405 nm was noted as function of irradiation time interval in min. Further, the changes in absorbance values against irradiation time was used to plot a relation Ln (A_0/A) versus irradiation time in min. This plot was studied to estimate the rate constant (k) value and further singlet oxygen quantum yield (Φ_Δ) for each synthesized porphyrin compound **3a-3i**. In this analysis, H_2TPP in DMF was used as a standard ($\Phi_\Delta = 0.64$). The singlet oxygen quantum yield (Φ_Δ) of photosensitizer **3a-3i** was determined by using **eq. 2** given below [16,18,20],

$$\Phi_\Delta = \Phi_{\Delta(ref)} \frac{A.\ k_{ref}}{A_{ref}.\ k} \tag{2}$$

where, Φ_Δ, $\Phi_{\Delta(ref)}$, k, k_{ref}, A and A_{ref} denotes singlet oxygen quantum yield of respective photosensitizer **3a-3i**, singlet oxygen quantum yield of reference H_2TPP, slope (rate constant) of kinetics of photooxidation of DMA by photosensitizer **3a-3i**, slope (rate constant) of kinetics of photooxidation of DMA by reference H_2TPP, absorbance of photosensitizer **3a-3i** and absorbance of reference H_2TPP, respectively.

Results and Discussion

Characteristics of Synthesized Porphyrin Analogues 3a-3i in IR, NMR and Mass Analysis

The target porphyrin analogues **3a-3i** were synthesized using a protocol as described in the experimental section. All the compounds were further analyzed for IR, NMR and mass spectroscopy to confirm their formation. The results for all the spectra analysis are given as supporting information (**Fig. S1- S27**). The appearance of characteristic broad band around 3400 cm^{-1} and sharp band around 1640–1650 cm^{-1} in IR spectrum of synthesized porphyrins **3a-3i** is because of -C-OH and -C=N stretching frequencies. While, appearance of two sharp bands around 3000–3050 cm^{-1} is due to the stretching of -C=NH. The proton NMR spectra of each porphyrin **3a-3i** show typical singlet peak around δ 10–12 ppm which clearly indicates presence of two -NH groups in the compound. In addition, presence of all -OH groups show singlet peak around δ 9–11 ppm in proton NMR spectra, while all other protons associated with the respective compounds fall within the aromatic region. The target porphyrin compounds were further supported by examining the mass spectrum of each compound. The mass spectrum of porphyrins **3a-3i** shows relevant M + 1, M + K or M + 4 molecular ion peak with respect to their molecular weight. Hence, IR,NMR and mass spectroscopy results confirms the formation of target porphyrin analogues **3a-3i** using present methodology. The detailed spectral analysis results of IR, NMR and mass studies is given as supporting information.

Photophysical Properties of Synthesized New Porphyrin Analogues 3a-3i

To investigate the photophysical properties such as absorption, fluorescence emission, fluorescence quantum yield and fluorescence lifetime for synthesized porphyrin analogues **3a-3i**, stock solutions of 10 μM concentrations of respective compounds were prepared in DMF. The absorption spectra were scanned within the wavelength range of 350–700 nm. Figure 1 shows absorption spectra of synthesized porphyrin analogues **3a-3i** in DMF at concentration of 10 μM each. The absorption spectra clearly indicate the change in absorption value as well as spectral shift in wavelength maxima of porphyrins **3a-3i** as compared to each other and reference H_2TPP. It is well known that compounds bearing porphyrin core shows typical absorption bands at shorter wavelength (Soret band) and longer wavelength (Q bands). Likewise, in present studies we found a characteristics behavior of absorption properties for synthesized porphyrin analogues **3a-3i** and those were comparable to reference compound H_2TPP. Principally, absorption spectra in Fig. 1 illustrate the bands in between 420 and 433 nm for compounds **3a-3i** are assigned as Soret bands. While, bands appearing to the longer absorption wavelength of 518–660 nm are stands for Q bands. The origin of these Soret and Q bands are due to the electronic transitions of $\pi \rightarrow \pi^*$. However, Soret and Q bands appeared at shorter and longer absorption wavelengths are arises due to electronic transitions occurred between ground state to higher singlet excited state and those are assigned as $S_0 \rightarrow S_2$ and $S_0 \rightarrow S_1$, respectively [18,21]. From the absorption spectra, it seems that *mono or di*--substituted halogen containing porphyrin compounds **3a, 3b, 3c, 3d** and **3h** induce hypsochromic shift in absorption wavelength maxima for both Soret and Q bands as compared to reference H_2TPP. While, non-halogenated porphyrin compounds slightly shift Soret and Q bands to longer wavelength from its maximum absorption wavelength as compared to H_2TPP. The effect of electron withdrawing capacity of halogen (**3a, 3b, 3c, 3d** and **3h**) and electron donating characters present in compound **3e** and **3f** might be the reason for hypsochromic and bathochromic shift observed for maximum absorption wavelength, respectively. However, compound **3g**

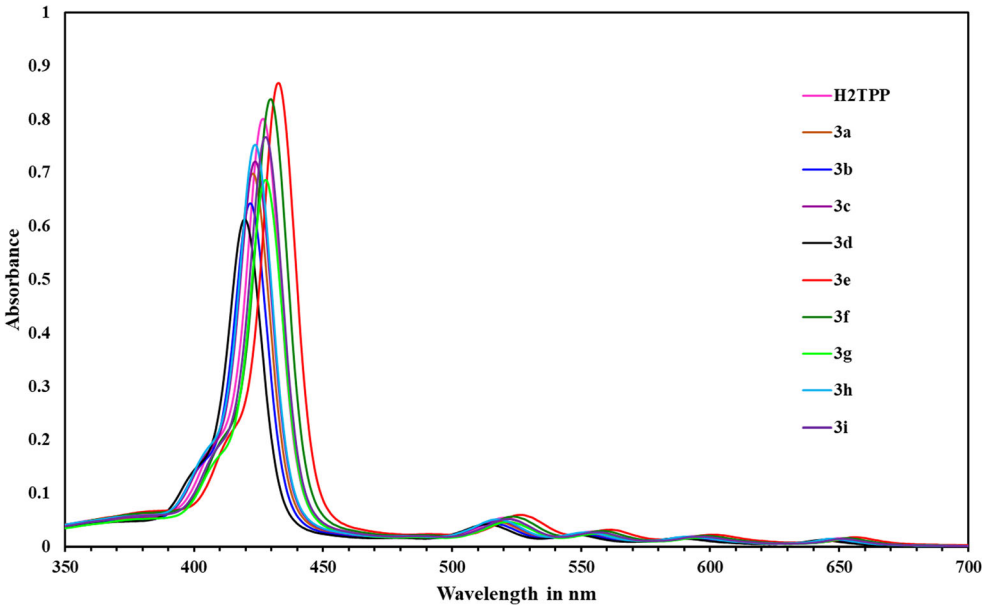

Fig. 1 Absorption spectra of synthesized porphyrin analogues **3a-3i** in DMF [10 μM]

shows unexceptional slight bathochromic shift even it contains electron withdrawing groups. Interestingly, all compounds show significant molar excitation coefficient values (ε) in DMF at respective wavelength maxima of Soret band. The estimated photophysical characteristics based on absorption studies such as assignment of Soret and Q bands along with the respective molar excitation coefficient values are given in Table 2.

Porphyrins are able to exhibit excellent fluorescence properties with emission at longer wavelength. Such fluorescence properties can be useful to estimate Stokes shift and further fluorescence lifetime values for respective porphyrins. Therefore, a 10 μM solution of each synthesized porphyrins **3a-3i** was examined for the measurement of respective fluorescence emission spectrum within the spectral range of 600–800 nm. For this purpose, each solution was triggered to its excitation wavelength of 420 nm. Figure 2 shows fluorescence emission spectra of synthesized porphyrins **3a-3i** in DMF at concentration of 10 μM. The significant fluorescence emission bands Q (0–0) and Q (0–1) were observed within the wavelength range of 644–660 and 708–725 nm, respectively. The returning of electronically excited singlet state (S_1) to ground state (S_0) through fluorescence emission is the reason for cause of fluorescence emission bands at individual Q bands [15,16,18]. The absorption and fluorescence properties are apparent to be coherent with each other as far as involvement of substituent groups in porphyrin structures. The same hypsochromic and bathochromic spectral shift trend was seen in case of maximum emission wavelength of porphyrins **3a-3i** with respect to reference H_2TPP. The enhanced fluorescence emission was seen in case of porphyrins **3e** and **3f** as compared with H_2TPP. The increase in fluorescence intensity for these two porphyrins attributes to presence of electron donating characters and restrictions of molecular

Table 2 Estimated photophysical properties of porphyrin analogues **3a-3i** in DMF

Porphyrin	λ_{soret} (nm)	$\varepsilon_{soret} \times 10^5$ (M^{-1} cm^{-1})	λ_{Qx} (0–0) (nm)	$\varepsilon_{Qx} \times 10^4$ (M^{-1} cm^{-1})	λ_{FL} Q(0–0) (nm)	λ_{FL} Q(0–1) (nm)	Stokes shift (nm)
H_2TPP	427	0.801	650	0.156	655	716	5
3a	423	0.697	647	0.136	651	713	4
3b	422	0.642	644	0.125	650	710	6
3c	424	0.720	648	0.141	652	713	4
3d	420	0.611	644	0.119	651	708	7
3e	433	0.868	657	0.170	660	725	3
3f	430	0.837	653	0.163	656	721	4
3g	428	0.685	644	0.134	650	711	6
3h	424	0.752	647	0.147	652	714	5
3i	428	0.766	649	0.150	653	714	4

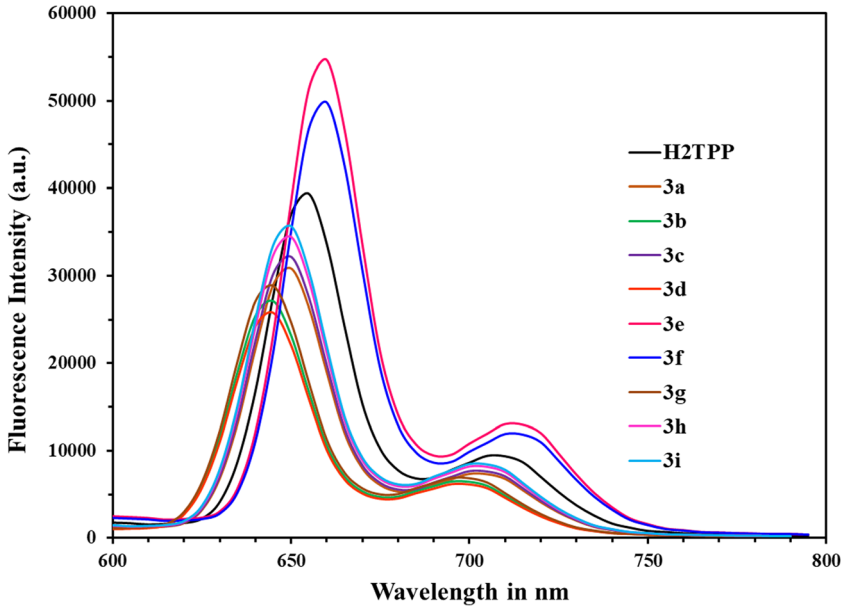

Fig. 2 Fluorescence emission spectra of synthesized porphyrin analogues **3a-3i** in DMF [10 μM]

rotations along with non-radiative decay pathways. While, a comparable emission response was observed for remaining porphyrin compounds. The Stokes shift represents the distinctive optical property. The estimated values of Stokes shifts for respective porphyrins **3a-3i** is the energy difference of fluorescence emission band Q (0–0) and absorption band Q_x (0–0). The significant Stokes shift values for porphyrins indicate strong intermolecular forces, low molecular rotations and increase in radiative pathways from excited state [18, 22–25]. Table 2 illustrates the observed maximum fluorescence emission bands and estimated Stokes shift values for porphyrins **3a-3i** in DMF at 10 μM concentration.

The other characteristic properties posed by any fluorescent compound generally known as fluorescence lifetime (τ_f) and fluorescence quantum yield (Φ_f). The average time spend by any excited fluorescent compound in its excited state is nothing but fluorescence lifetime of that compound. Such fluorescence lifetime values are helpful to interpret the state of existence and interactions of compound in its excited state. In present investigations, all the porphyrins **3a-3i** were subjected to examine for their fluorescence decay by using time-correlated single photon counting (TCSPC) method and excitation wavelength used was 420 nm. The porphyrins having electron donating groups in their structures show slightly higher fluorescence lifetime values as compared to reference compound H_2TPP. However, analogous values were seen in case of porphyrins containing electron withdrawing groups and H_2TPP. The fluorescence lifetime values for synthesized porphyrins **3a-3i** were estimated on Data station software attached with TCSPC spectrophotometer (HORIBA-iHR320) and given in Table 3. Along with fluorescence lifetime values, fluorescence quantum yields (Φ_f) frequently used to examine the efficiency of intersystem crossing for compound to the triplet excited state. This is a crucial phase in $^1O_2$ generation. Therefore, fluorescence quantum yields were calculated comparative to reference H_2TPP. The calculated fluorescence quantum yield values for synthesized porphyrins **3a-3i** are given in Table 3. The variable fluorescence quantum yield values were received for porphyrins **3a-3i**. Table 3 illustrate porphyrins with electron withdrawing substituents in their structures have lower value of fluorescence lifetime as well as fluorescence quantum yield. While, porphyrins with electron donating characters show opposite trends for fluorescence lifetime and quantum yield values. The lower values of fluorescence quantum yield indicate significant deactivation of singlet excited state through the other fluorescence competing processes such as intersystem crossing to the triplet excited state. The synthesized porphyrins **3a, 3b, 3c, 3d, 3g, 3h** and **3i** show lower fluorescence lifetime and quantum yield

Table 3 Fluorescence lifetime (τ_f) and fluorescence quantum yield (Φ_f) of porphyrin analogues **3a-3i** in DMF

Compound	Fluorescence lifetime τ_f (ns)	Fluorescence quantum yield (Φ_f)
H_2TPP	8.25	0.12
3a	6.16	0.17
3b	6.12	0.15
3c	6.17	0.18
3d	6.11	0.14
3e	9.37	0.22
3f	8.96	0.20
3g	6.14	0.16
3h	6.20	0.18
3i	6.22	0.18

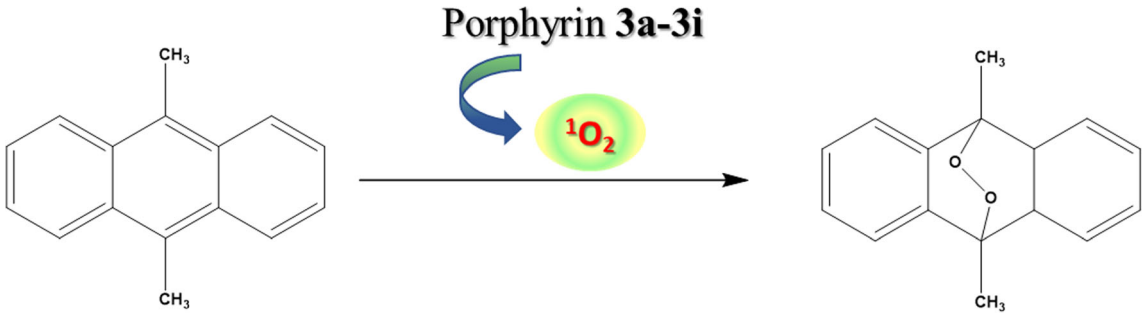

Fig. 3 Formation of endoperoxide by reaction of DMA and photosensitizer able to generate $^1O_2$

values than **3e** and **3f**. The compounds **3b, 3d** and **3g** have lowest values for fluorescence lifetime and quantum yield since both contains higher electron withdrawing characters than any other synthesized porphyrins.

Singlet Oxygen Quantum Yield of Synthesized New Porphyrin Analogues 3a-3i

There are variety of methods available to estimate the singlet oxygen quantum yield (Φ_Δ) of photosensitizers. The photooxidation of DMA in the presence of suitable photosensitizer is commonly used method to evaluate the efficiency of singlet oxygen generation in terms of singlet oxygen quantum yield. The change in absorbance of DMA at 402 nm was monitored separately in the presence of synthesized porphyrins **3a-3i** as photosensitizer. Initially, the absorbance of DMA was seen maximum at 402 nm which is distinctive than Soret band of synthesized porphyrins. In the presence of photosensitizers **3a-3i**, absorbance of DMA decreases as the time of irradiation increases from 0 to 60 min. The rapid reaction between generated singlet oxygen ($^1O_2$) from photosensitizer **3a-3i** and DMA led to form endoperoxide which further accountable for the consecutive decrease in the absorbance value of DMA at 402 nm. Figure 3 represents formation of endoperoxide of DMA by the reaction of singlet oxygen ($^1O_2$) generated by photosensitizer and DMA. This photooxidation process of DMA in the presence of suitable photosensitizer **3a-3i** follows pseudo first-order kinetics [16, 26–28] which was examined by plotting linear square fit of Ln (A_0/A) as function of irradiation time in min and given as Fig. 4. The rate equation used to plot kinetics for the photooxidation reaction of DMA is given below as **eq. 3**,

$$Ln\frac{A_0}{A} = kt \tag{3}$$

where, A_0, A, k and t represents the initial absorbance value of photosensitizer, absorbance value of photosensitizer at particular irradiation time, first order rate constant and irradiation time in min, respectively. The slope value of photooxidation of DMA by each photosensitizer **3a-3i** represents value of rate constant 'k'. This obtained value of rate constant 'k' was further used to calculate the singlet oxygen quantum yield (Φ_Δ) of each synthesized porphyrin photosensitizer **3a-3i**. Table 4 shows values of observed

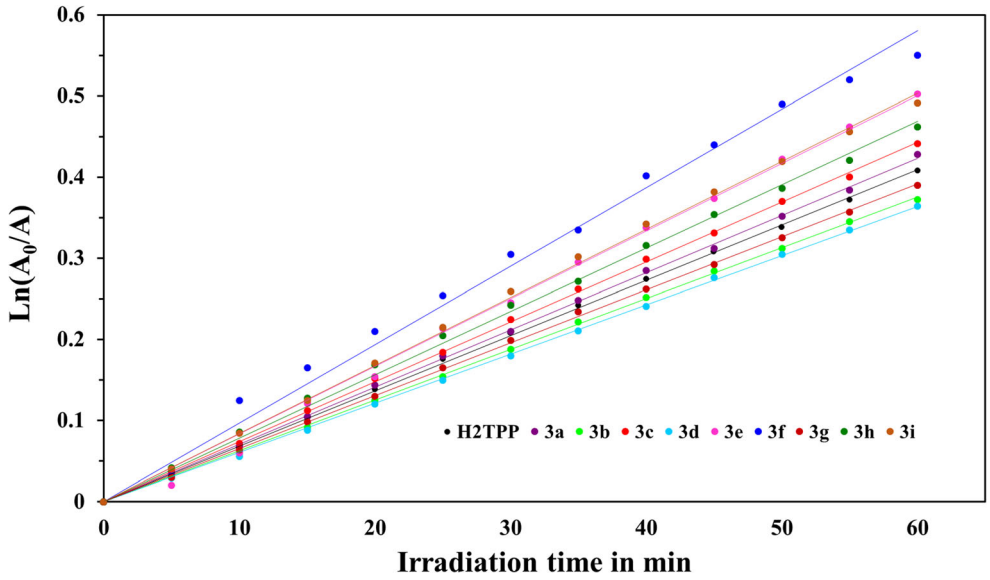

Fig. 4 Plot of kinetics of photooxidation of DMA by photosensitizers **3a-3i**

Table 4 Rate constant (k) for photooxidation of DMA and Singlet oxygen quantum yield (Φ_Δ) for porphyrin analogues **3a-3i** in DMF

Compound	Rate constant (k) min^{-1}	Singlet oxygen quantum yield (Φ_Δ)
3a	0.0071	0.61
3b	0.0063	0.64
3c	0.0074	0.59
3d	0.0061	0.66
3e	0.0085	0.52
3f	0.0097	0.54
3g	0.0065	0.62
3h	0.0078	0.58
3i	0.0084	0.56

rate constant (k) and singlet oxygen quantum yield (Φ_Δ) for respective porphyrins **3a**-**3i**. The value of Φ_Δ was found to be in the range of 0.52 to 0.66 for porphyrins **3a-3i** as compared to the reference H_2TPP ($\Phi_\Delta = 0.64$). This experiment shows porphyrins with electron withdrawing characters exhibit either highest or comparable value of Φ_Δ than reference H_2TPP. While, other porphyrins such as **3e** and **3f** bearing electron donating characters in their structures present lower Φ_Δ values than reference H_2TPP. Interestingly, it was found that increase in the electron withdrawing characters increase the Φ_Δ values for porphyrins **3b, 3d** and **3g** as compared to reference H_2TPP and porphyrins **3a, 3c, 3h** and **3i**. Thus, in an overall studies on photophysical properties and singlet oxygen quantum yields suggest synthesized porphyrins **3b, 3d** and **3g** could be the potent candidature as PDT agents. While, porphyrins **3a, 3c, 3h** and **3i** show comparably significant efficiency for the singlet oxygen generation when compared to reference H_2TPP.

Photostability of Synthesized New Porphyrin Analogues 3a-3i

A stable and good photosensitizer should not deviate its absorbance in dark condition and thus displays its photostability [15,18,27]. To examine the photostability of said porphyrins **3a-3i**, the solutions of all synthesized porphyrins under studies were kept in dark condition for the period of 90 days. The examination of absorbance after the 90 days does not affect the initial absorbance value for porphyrins **3a-3i**. In addition, the all porphyrin solutions recovered after dark conditions of 90 days are free from any agglomeration, sedimentation or aggregation. Therefore, considering all these observations during the present investigation guide us to conclude that synthesized all porphyrins are photostable and some of them have potency to be a PDT agent.

Conclusion

New porphyrin analogues were synthesized and characterized by using analytical techniques such as IR, NMR and Mass spectroscopies. The analysis of absorption, fluorescence emission, fluorescence lifetime and fluorescence quantum yield for synthesized porphyrins **3a-3i** suggests analogous and enhanced photophysical properties for some of porphyrins when compared to reference H_2TPP. The synthesized porphyrins **3a-3i** were examined for their application as PDT agent through the studies on photooxidation of DMA. The estimation of singlet oxygen quantum yield for porphyrins **3a-3i** illustrate the more electron withdrawing characters in the compound responsible for the increases in the singlet oxygen quantum yield in case of porphyrins **3b, 3d** and **3g** as compared to reference H_2TPP and remaining porphyrins. However, all synthesized porphyrins have comparable potency for the generation of singlet oxygen relative to reference H_2TPP. Pleasingly, photostability of synthesized porphyrins was found to be excellent over the period of 90 days. In conclusion, porphyrins **3b, 3d** and **3g** possessing akin photophysical properties and higher singlet oxygen quantum yield values as compared to reference H_2TPP can be utilized as templates in the development of PDT agents.

Acknowledgements This research was supported by Basic Science Research Program through the National Research Foundation of Korea (NRF) funded by the Ministry of Education (NRF- 2019R1I1A3A01059089).

References

1. Fayter D, Corbett M, Heirs M, Fox D, Eastwood A (2010) A systematic review of photodynamic therapy in the treatment of pre-cancerous skin conditions, Barrett's oesophagus and cancers of the biliary tract, brain, head and neck, lung, oesophagus and skin, health Technol. Assess 14:1–288
2. Sunar U (2013) Monitoring photodynamic therapy of head and neck malignancies with optical spectroscopies. World J Clin Cases 1:96–105
3. Liu Y, Wang W, Jianhong Y, Zhou C, Sun J (2013) pH-sensitive polymeric micelles triggered drug release for extracellular and intracellular drug targeting delivery. Asian J Pharmaceu Sci 8:159–167
4. Shafirstein G, Battoo A, Harris K, Baumann H, Gollnick SO, Lindenmann J, Nwogu CE (2016) Photodynamic therapy of non-small cell lung Cancer. Narrative review and future directions. Ann Am Thorac Soc 13:265–275
5. Agostinis P, Berg K, Cengel KA, Foster TH, Girotti AW, Gollnick SO, Hahn SM, Hamblin MR, Juzeniene A, Kessel D (2011) Photodynamic therapy of cancer: an update. CA Cancer J Clin 61:250–281
6. Brown SB, Brown EA, Walker I (2004) The present and future role of photodynamictherapy in cancer treatment. Lancet Oncol 5:497–508

7. Jang B, Choi Y (2012) Photosensitizer-conjugated gold Nanorods for enzyme-Activatable fluorescence imaging and photodynamic therapy. Theranostics 2:190–197
8. Henderson BW, Dougherty TJ (1992) How does photodynamic therapy work? Photochem Photobiol 155:145–157
9. Josefsen LB, Boyle RW (2012) Unique diagnostic and therapeutic roles of porphyrins and phthalocyanines in photodynamic therapy, imaging and theranostics. Theranostics 2:916–966
10. Bhaumik J, Gogia G, Kirar S, Vijay L, Thakur NS, Banerjee UC, Laha JK (2016) Bioinspired nanophotosensitizers: synthesis and characterization of porphyrin–noble metal nanoparticle conjugates. New J Chem 40:724–731
11. Scalise I, Durantini EN (2004) Photodynamic effect of metallo 5-(4-carboxyphenyl)-10,15,20-tris(4-methylphenyl) porphyrins in biomimetic AOT reverse micelles containing urease. J Photochem Photobiol A 162:105–113
12. Johnson-White B, Zeinali M, Shaffer KM, Patterson CH, Charles PT, Markowitz MA (2007) Detection of organics using porphyrin embedded nanoporous organosilicas. Biosens Bioelectron 22: 1154–1162
13. Jeong EY, Burri A, Lee S, Park SE (2010) Synthesis and catalytic behavior of tetrakis(4-carboxyphenyl) porphyrin-periodic mesoporous organosilica. J Mater Chem 20:10869–10875
14. Peng Q, Moan J, Ma LW, Nesland JM (1995) Uptake, localization, and photodynamic effect of meso-tetra(hydroxyphenyl)porphine and its corresponding chlorin in normal and tumor tissues of mice bearing mammary carcinoma. Cancer Res 55:2620–2626
15. Rojkiewicz M, Kus P, Kozub P, Kempa M (2013) The synthesis of new potential photosensitizers [1]. Part 2. Tetrakis-(hydroxyphenyl) porphyrins with long alkyl chain in the molecule. Dyes Pigments 99:627–635
16. Ormond AB, Freeman HS (2013) Effects of substituents on the photophysical properties of symmetrical porphyrins. Dyes Pigments 96:440–448
17. Spesia MB, Lazzeri D, Pascual L, Rovera M, Durantini EN (2005) Photoinactivation of *Escherichia coli* using porphyrin derivatives with different number of cationic charges. FEMS Immunol Med Microbiol 44:289–295
18. Mahajan PG, Dige NC, Vanjare BD, Phull AR, Kim SJ, Hong SK, Lee KH (2018) Synthesis, photophysical properties and application of new porphyrin derivatives for use in photodynamic therapy and cell imaging. J Fluoresce 28:871–882
19. Nifiatis F, Athas JC, Gunaratne KDD, Gurung Y, Monette KM, Shivokevich PJ (2011) Substituent effect of porphyrin on singlet oxygen generation quantum yields. The Open Spectroscopy Journal 5:1–12
20. Mahajan PG, Dige NC, Vanjare BD, Raza H, Mubashir H, Seo SY, Kim CY, Lee KH (2019) Facile synthesis of new quinazolinone benzamides as potent tyrosinase inhibitors: comparative spectroscopic and molecular docking studies. J Mol Struc 1198:126915
21. Uttamlal M, Holmes-Smith AS (2008) The excitation wavelength dependent fluorescence of porphyrins. Chem Phys Lett 454:223–228
22. Sun X, Zhang J, He B (2005) The synthesis and photochemical characterization of mesotetra-thienyl porphyrins. J Photochem Photobio A: Chem 172:283–288
23. Ha JH, Ko S, Lee CH, Lee CY, Kim YR (2001) Effect of core atom modification on photophysical properties and singlet oxygen generation efficiencies: tetraphenylporphyrin analogues core-modified by oxygen and/or sulfur. Chem Phys Lett 349:271–278
24. Mahajan PG, Dige NC, Desai NK, Patil SR, Kondalkar VV, Hong SK, Lee KH (2018) Selective detection of Co^{2+} by fluorescent nano probe: Diagostic approach for analysis of environmental samples and biological activities. Spectrochim Acta A: Mol Biomol Spectro 198:136–144
25. Dige NC, Mahajan PG, Dhokale RK, Chinchkar SM, Patil MV, Pore DM (2019) Novel route for the synthesis of 5-(4-Hydroxy-2-oxo-2*H*-chromen-3-yl)-1,3-dimethyl-1*H*-chromeno[2,3-*d*-]pyrimidine-2,4(3*H*,5*H*)-diones. Org Prep Proced Int 51:553–565
26. Serra AC, Pineiro M, Rocha Gonsalves A, Abrantes M, Laranjo M, Santos AC (2008) Halogen atom effect on photophysical and photodynamic characterisics of derivatives of 5,10,15,20-tetrakis(3-hydroxyphenyl)porphyrin. J Photochem Photobio B: Biology 92: 59–65
27. Mahajan PG, Dige NC, Vanjare BD, Eo SH, Seo SY, Kim SJ, Hong SK, Choi CS, Lee KH (2019) A potential mediator for photodynamic therapy based on silver nanoparticles functionalized with porphyrin. J Photochem Photobio A Chemistry 377:26–35
28. Mahajan PG, Dige NC, Vanjare BD, Phull AR, Kim SJ, Lee KH (2019) Gallotannin mediated silver colloidal nanoparticles as multifunctional nano platform: rapid colorimetric and turn-on fluorescent sensor for Hg^{2+}, catalytic and *In vitro* anticancer activities. J Lumin 206:624–633